Inorg. Chem. **2009**, *48*, 2507−2517

Dinitrogen Complexes Supported by Tris(phosphino)silyl Ligands

Matthew T. Whited,[†] Neal P. Mankad, Yunho Lee, Paul F. Oblad,[†] and Jonas C. Peters*

Department of Chemistry, Massachusetts Institute of Technology, Cambridge, Massachusetts 02139

Received September 29, 2008

The tetradentate tris(phosphino)silyl ligand $[SiP^{iPr}_3]$ ($[SiP^{iPr}_3] = [Si(o\text{-}C_6H_4P^iPr_2)_3]^-$) has been prepared, and its complexation with iron, cobalt, nickel, and iridium precursors has been explored. Several coordination complexes have been thoroughly characterized and are described. These include, for example, the divalent trigonal bipyramidal metal chlorides $[SiP^{iPr}_3]M-Cl$ (M = Fe, Co, Ni), as well as the monovalent dinitrogen adducts $[SiP^{iPr}_3]M-N_2$ (M = Fe, Co, Ir), which are compared with related $[SiP^{Ph}_3]M-Cl$ and $[SiP^{Ph}_3]M-N_2$ species (M = Fe, Co). Complexes of this type represent the first examples of terminal dinitrogen adducts of monovalent iron, and the ligand architecture allows examination of a unique class of dinitrogen adducts with a *trans*-disposed silyl donor. Oxidation of the appropriate $[SiP^R_3]M-N_2$ precursors affords the divalent iron triflate $[SiP^{Ph}_3]Fe(OTf)$ and trivalent cobalt triflate $\{[SiP^{iPr}_3]Co(OTf)\}\{OTf\}$ complexes, which are of interest for group transfer studies because of the presence of a labile triflate ligand. Comparative electrochemical, structural, and spectroscopic data are provided for these complexes.

I. Introduction

A great deal of biochemical, theoretical, and synthetic research has recently been focused on exploring the nature of the inorganic cofactors of nitrogenase enzymes.[1,2] Given the presence of iron and molybdenum in FeMo-nitrogenase, particular emphasis has been placed on elucidating the roles these elements may play in N_2 reduction.[2,3] Yandulov and Schrock recently reported a catalytic cycle for N_2 reduction involving a trivalent triamidoamine $[NN_3]Mo-N_2$ species that is thought to shuttle between four different formal oxidation states.[4]

We and others have established that, given a suitable set of supporting ligands, single low-coordinate iron sites can exhibit the necessary redox flexibility to facilitate multielectron small molecule reductions,[5,6] and we have begun to target a synthetic scheme akin to the Chatt cycle in which a monovalent iron center binds N_2 and mediates its reduction via proton/electron equivalents.[2,6,7] In this context it is interesting to consider terminal Fe^I-N_2 complexes as synthetic targets. Our group and Holland's group have reported the preparation of μ-N_2 complexes of three- and four-coordinate iron in which the iron centers may be formally regarded as iron(I).[5d,f] More detailed spectroscopic studies have suggested that the Holland system, supported by β-diketiminato ligands, is perhaps better described as a diiron(II) species with a reduced dinitrogen dianion.[8] In contrast, our phosphine-supported diiron system appears to be better described by two $S = 3/2$ iron centers that are very weakly ferromagnetically coupled.[6]

* To whom correspondence should be addressed. E-mail: jcpeters@mit.edu.

[†] California Institute of Technology, Pasadena, CA 91125.

(1) (a) Howard, J. B.; Rees, D. C. *Chem. Rev* **1996**, *96*, 2965; Burgess, B. K., Lowe, D. J. *Chem. Rev.* **1996**, *96*, 2983. (b) Chatt, J.; Dilworth, J. R.; Richards, R. L. *Chem. Rev.* **1978**, *78*, 589.

(2) Peters, J. C.; Mehn, M. P. In *Activation of Small Molecules*; Tolman, W. B., Ed.; Wiley: New York, 2006; pp 81−120.

(3) MacKay, B. A.; Fryzuk, M. D. *Chem. Rev.* **2004**, *104*, 385.

(4) (a) Yandulov, D. V.; Schrock, R. R. *Science* **2003**, *301*, 76. (b) Yandulov, D. V.; Schrock, R. R. *J. Am. Chem. Soc.* **2002**, *124*, 6252. (c) Schrock, R. R. *Acc. Chem. Res.* **2005**, *38*, 955.

(5) (a) Brown, S. D.; Betley, T. A.; Peters, J. C. *J. Am. Chem. Soc.* **2003**, *125*, 322. (b) Brown, S. D.; Peters, J. C. *J. Am. Chem. Soc.* **2005**, *127*, 1913. (c) Brown, S. D.; Mehn, M. P.; Peters, J. C. *J. Am. Chem. Soc.* **2005**, *127*, 13146. (d) Betley, T. A.; Peters, J. C. *J. Am. Chem. Soc.* **2003**, *125*, 10782. (e) Betley, T. A.; Peters, J. C. *J. Am. Chem. Soc.* **2004**, *126*, 6252. (f) Smith, J. M.; Lachicotte, R. J.; Pittard, K. A.; Cundari, T. R.; Lukat-Rodgers, G.; Rodgers, K. R.; Holland, P. L. *J. Am. Chem. Soc.* **2001**, *123*, 9222. (g) Holland, P. L. *Can. J. Chem.* **2005**, *83*, 296. (h) Smith, J. M.; Sadique, A. R.; Cundari, T. R.; Rodgers, K. R.; Lukat-Rodgers, G.; Lachicotte, R. J.; Flaschenriem, C. J.; Vela, J.; Holland, P. L. *J. Am. Chem. Soc.* **2006**, *128*, 756.

(6) Hendrich, M. P.; Gunderson, W.; Behan, R. K.; Green, M. T.; Mehn, M. P.; Betley, T. A.; Lu, C. C.; Peters, J. C. *Proc. Natl. Acad. Sci. U.S.A.* **2006**, *103*, 17107.

(7) MacBeth, C. E.; Harkins, S. B.; Peters, J. C. *Can. J. Chem.* **2005**, *83*, 332.

(8) Stoian, S. A.; Vela, J.; Smith, J. M.; Sadique, A. R.; Holland, P. L.; Munck, E.; Bominaar, E. L. *J. Am. Chem. Soc.* **2006**, *128*, 10181.

10.1021/ic801855y CCC: $40.75
Published on Web 02/11/2009

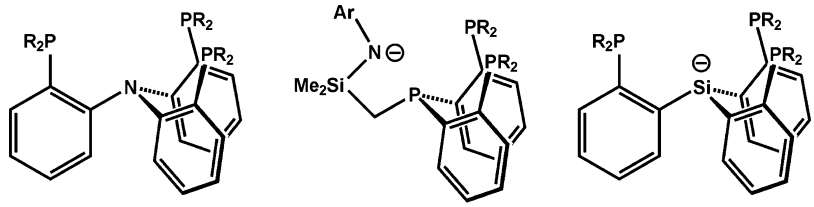

Figure 1. Neutral and anionic tetradentate ligands related to the chemistry described herein.

We have recently begun to consider whether monoanionic tetradentate ligands might stabilize *terminally* bonded N_2 adducts of monovalent iron. Accordingly, we have explored two complementary approaches to introduce a single X-type donor into a phosphine-rich, tetradentate framework (Figure 1).[9,10] Recent results have established that tris(phosphino)silyl ligands (abbreviated in general as [SiP^R_3]) are promising scaffolds for the examination of N_2 chemistry at iron.[9b] Ligands of this type, the sole example of which was first reported by Stobart,[11] are also of general interest for catalytic studies since the presence of a strongly *trans*-influencing silyl donor should labilize bound substrates to facilitate turnover.

Herein we discuss the preparation and characterization of the isopropyl-substituted [SiP^{iPr}_3] ligand derivative and probe aspects of its fundamental coordination chemistry with di- and trivalent iron, cobalt, nickel, and iridium. We present complementary strategies for metalation of the silane ligand and examine the monovalent, terminal dinitrogen complexes [SiP^{iPr}_3]M$-N_2$ (M = Fe, Co, Ir). Comparisons are made where informative to related [SiP^{Ph}_3] systems.[9b]

II. Results and Discussion

Synthesis and Characterization of H[SiP^{iPr}_3]. (2-Bromophenyl)phosphines serve as excellent precursors for a variety of phosphine ligands since they are readily lithiated with a single equivalent of *n*-butyllithium in diethyl ether at low temperature.[9a,12] Although the (2-bromophenyl)diphenylphosphine precursor required for the synthesis of H[SiP^{Ph}_3] is most easily obtained by a Pd-catalyzed coupling reaction,[9a,13] we were unable to access the diisopropylphosphine derivative by such a route, and it was instead synthesized by the addition of ^{i}PrMgCl to the previously reported (2-bromophenyl)dichlorophosphine.[14] To prepare the desired silane, 2-(diisopropylphosphino)phenyllithium was generated at low temperature and isolated without further purification as an orange solid. Quenching this lithio species with 1/3 equivalent of trichlorosilane in toluene, followed by heating at 90 °C, afforded the target H[SiP^{iPr}_3] ligand (**1**, Scheme 1). Combustion analysis, ^{1}H and ^{31}P NMR spectroscopy, and an X-ray diffraction (XRD) study confirm the assignment of the desired silane. The silyl proton is obscured by aromatic proton resonances in the ^{1}H NMR spectrum. However, the Si$-$H vibration (υ_{SiH} = 2218 cm^{-1}) is prominent in the infrared spectrum and provides a convenient handle with which to monitor consumption of the silane ligand during metalation reactions (vide infra). The solid-state molecular structure of **1** obtained by XRD analysis (Scheme 1) reveals an arrangement in which the phosphine arms adopt a propeller structure trisected by the Si$-$H unit with the H-atom approximately equidistant from each P atom (P$-$H$_{Si}$(avg.) = 3.14(2) Å), suggesting a convenient metal binding site upon substitution of the silyl proton by a transition metal ion. The P$-$H$_{Si}$ distances are sufficiently long that no interaction in the solid state can be inferred.

Scheme 1

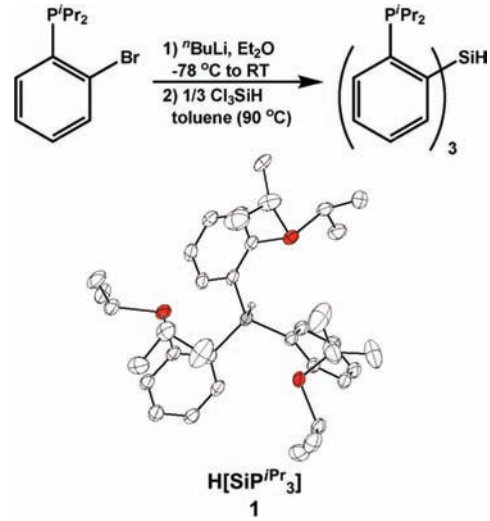

Synthesis and Characterization of Di- and Trivalent [SiP^{iPr}_3]M Complexes. Metalation of polydentate silyl ligands has often been accomplished via chelate-assisted Si$-$H bond oxidative addition at late metal precursors.[15] This method is a straightforward route for installing the [SiP^{iPr}_3] ligand on Co, Ni, and Ir precursors, as shown in Scheme 2.

(9) (a) Whited, M. T.; Rivard, E.; Peters, J. C. *Chem. Commun.* **2006**, 1613. (b) Aspects of the current work have been previously communicated: Mankad, N. P.; Whited, M. T.; Peters, J. C. *Angew. Chem., Int. Ed.* **2007**, *46*, 5768.

(10) Arnold and coworkers have recently adopted a similar approach in their synthesis of monoanionic, tetradentate ligands: (a) Chomitz, W. A.; Arnold, J. *Chem. Commun.* **2007**, 4797. (b) Chomitz, W. A.; Mickenberg, S. F.; Arnold, J. *Inorg. Chem.* **2008**, *47*, 373.

(11) Joslin, F. L.; Stobart, S. R. *J. Chem. Soc., Chem. Commun.* **1989**, 504.

(12) Mankad, N. P.; Rivard, E.; Harkins, S. B.; Peters, J. C. *J. Am. Chem. Soc.* **2005**, *127*, 16032.

(13) Brauer, D. J.; Hingst, M.; Kottsieper, K. W.; Liek, C.; Nickel, T.; Tepper, M.; Stelzer, O.; Sheldrick, W. S. *J. Organomet. Chem.* **2002**, *645*, 14.

(14) Talay, R.; Rehder, D. *Zeit. Naturforsch., B: Anorg. Chem.* **1981**, *36*, 451.

(15) (a) Grundy, S. L.; Holmessmith, R. D.; Stobart, S. R.; Williams, M. A. *Inorg. Chem.* **1991**, *30*, 3333. (b) Okazaki, M.; Ohshitanai, S.; Iwata, M.; Tobita, H.; Ogino, H. *Coord. Chem. Rev.* **2002**, *226*, 167. (c) Gossage, R. A.; McLennan, G. D.; Stobart, S. R. *Inorg. Chem.* **1996**, *35*, 1729.

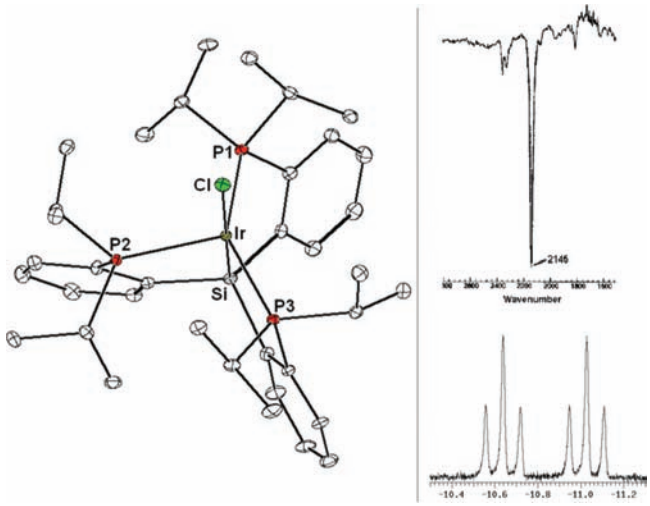

Figure 2. Displacement ellipsoid (35%) representation of [SiP$^{iPr}_3$]Ir(H)(Cl) (**4**) with inset of IR stretch and ^{1}H NMR signal for the Ir−*H*. Hydrogen atoms and a molecule of benzene have been omitted for clarity. Selected bond distances (Å) and angles (deg): Ir−Si 2.2749(8), Ir−P1 2.3597(8), Ir−P2 2.3848(8), Ir−P3 2.3151(8), Ir−Cl 2.5433(7), P1−Ir−P2 107.43(3), P1−Ir−P3 145.05(3), P2−Ir−P3 103.95(3), Si−Ir−Cl 178.46(3).

Scheme 2

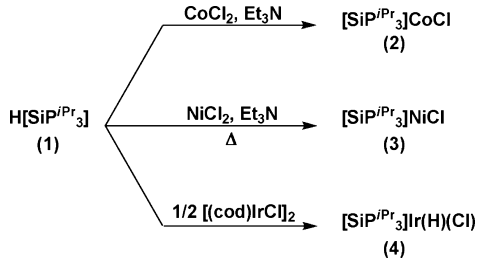

For instance, monitoring a slurry of either $CoCl_2$ or $NiCl_2$ in the presence of the neutral silane **1** and a sacrificial amine base (e.g., Et_3N or $^iPr_2NEt$) by IR spectroscopy established the gradual decay of the Si−H vibration over a period of 16 h for $CoCl_2$ at ambient temperature and 12 h for $NiCl_2$ in refluxing tetrahydrofuran (THF). By this method red [SiP$^{iPr}_3$]CoCl (**2**) and pale red [SiP$^{iPr}_3$]NiCl (**3**) could be isolated in analytically pure form and high yields (80% and 96%, respectively). The presence of a single resonance (δ 35.6 ppm) in the ^{31}P NMR spectrum of diamagnetic complex **3** suggested a C_3-symmetric solution structure, and XRD analysis confirmed this assignment for both **2** and **3** in the solid state (Figure 3).

A potentially useful iridium synthon was prepared by the addition of **1** to a stirring solution of orange $[(cod)IrCl]_2$ (cod = 1,4-cyclooctadiene), providing after 12 h the pale yellow complex [SiP$^{iPr}_3$]Ir(H)(Cl) (**4**) in 95% yield. A single crystal of **4** was analyzed by XRD methods. The hydride was not located in the difference map, but its presence was indicated by infrared spectroscopy ($\upsilon_{Ir-H} = 2145$ cm^{-1}). The distinctive hydride signal observed by ^{1}H NMR at δ −10.83 ppm (dt, $^2J_{HP(trans)} = 118$ Hz, $^2J_{HP(cis)} = 24$ Hz) reveals coupling to two inequivalent ^{31}P nuclei, and in combination with XRD data this suggests a geometry in which the chloride ligand is situated *trans* to the silyl donor and the hydride ligand sits in the plane of the three phosphines, *trans* to one and *cis* to the other two (Figure 2). This complex is similar to octahedral iridium(III) hydrido chloride complexes of chelating silyl ligands previously reported, in which the weakly *trans*-influencing chloride ligand prefers the site opposite the silyl donor.[15c]

Installation of the silyl ligand at iron precursors in high yield proved more challenging. For instance, the reaction of **1** with Fe_2Mes_4 (Mes = 2,4,6-trimethylphenyl), which proved successful in the preparation of [SiP$^{Ph}_3$]Fe(Mes),[9b] gave rise to an ill-defined reaction mixture from which [SiP$^{iPr}_3$]Fe(Mes) could not be readily isolated. The reaction of **1** with a single equivalent of ferrous chloride in THF generated the bis(phosphine) adduct complex (H[SiP$^{iPr}_3$])$FeCl_2$ (**5**), whose structure was established by X-ray crystallography (Scheme 3). For comparison, the phenyl-substituted derivative H[SiP$^{Ph}_3$] did not react with $FeCl_2$ under similar conditions. No dehydrohalogenation was observed upon exposure of **5** to amine bases such as Et_3N, even at elevated temperatures. To induce successful activation of the Si−H unit and thus install the desired Fe−Si bond we explored the generation of a mixed alkyl-chloride complex, akin to those examined by Kauffmann and co-workers,[16] hoping that alkane elimination might drive Fe−Si bond formation. Slow dropwise addition of MeMgCl to a stirring solution of **5** at −78 °C led to an immediate color change from pale yellow to bright orange, characteristic of the trigonal bipyramidal [SiP$^{iPr}_3$]FeCl (**6**, Scheme 3). The chloride complex **6** has been prepared in a one-pot synthesis in respectable yield (43%) first by addition of H[SiP$^{iPr}_3$] to $FeCl_2$ at room temperature, followed by cooling and addition of the Grignard reagent. This method of installing the H[SiP$^{iPr}_3$] ligand appears to be of broad utility and can also be used for the independent synthesis of [SiP$^{Ph}_3$]FeCl (**8**), as has been previously noted.[9b]

The solution magnetic moments and solid-state structural data (Figure 3) for the [SiP$^{iPr}_3$]M−Cl complexes (Fe, Co, Ni) indicate that the ligand confers a preference for trigonal bipyramidal geometries at later first row metals, in contrast to several previously reported, potentially tetradentate ligands that show a tendency to dissociate a donor to accommodate higher spin states with four-coordinate geometries.[7,9a,17] The spin states of the divalent iron (triplet, $\mu_{eff} = 3.3\ \mu_B$), cobalt (doublet, $\mu_{eff} = 1.8\ \mu_B$), and nickel (singlet) chloride complexes are in accord with the expected d-orbital splitting pattern for trigonal bipyramidal complexes supported by strong-field donor sets.[18]

Compared to our series of previously reported 4-coordinate tris(phosphino)borate [PhBP$^R_3$]M−X complexes (M = Mn,[19] Fe,[5a,20] Co,[21] Ni[22]), the presence of the silyl donor draws the coordinated metal ion into the plane of the three

(16) Kauffmann, T.; Laarmann, B.; Menges, D.; Neiteler, G. *Chem. Ber. Recl.* **1992**, *125*, 163.
(17) (a) Sacconi, L.; Divaira, M. *Inorg. Chem.* **1978**, *17*, 810. (b) Stoppioni, P.; Mani, F.; Sacconi, L. *Inorg. Chim. Acta* **1974**, *11*, 227.
(18) Cotton, F. A. *Chemical Applications of Group Theory*, 3rd ed.; Wiley: New York, 1990.
(19) Lu, C. C.; Peters, J. C. *Inorg. Chem.* **2006**, *45*, 8597.
(20) Betley, T. A.; Peters, J. C. *Inorg. Chem.* **2003**, *42*, 5074.
(21) (a) Shapiro, I. R.; Jenkins, D. M.; Thomas, J. C.; Day, M. W.; Peters, J. C. *Chem. Commun.* **2001**, 2152. (b) Jenkins, D. M.; Di Bilio, A. J.; Allen, M. J.; Betley, T. A.; Peters, J. C. *J. Am. Chem. Soc.* **2002**, *124*, 15336. (c) Jenkins, D. M.; Peters, J. C. *J. Am. Chem. Soc.* **2005**, *127*, 7148.

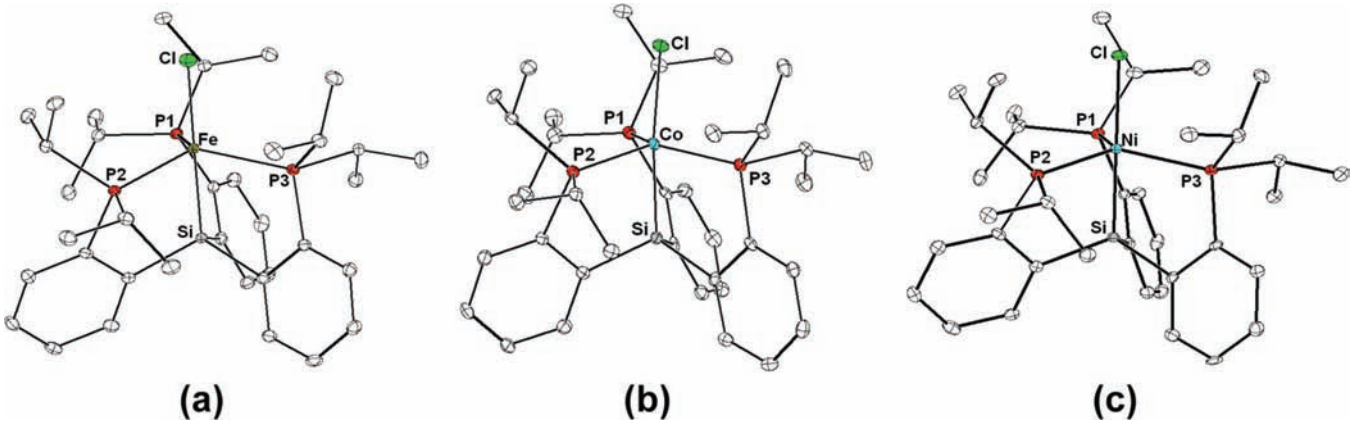

Figure 3. Displacement ellipsoid (35%) representations of (a) [SiP$^{iPr}_3$]FeCl (**6**), (b) [SiP$^{iPr}_3$]CoCl (**2**), and (c) [SiP$^{iPr}_3$]NiCl (**3**). Solvent molecules and hydrogen atoms have been omitted for clarity. Selected bond distances (Å) and angles (deg), for **5**: Fe−Si 2.305(1), Fe−P1 2.3627(7), Fe−P2 2.3438(7), Fe−P3 2.3489(7), Fe−Cl 2.2820(9), P1−Fe−P2 115.67(2), P1−Fe−P3 116.70(2), P2−Fe−P3 118.09(2), Si−Fe−Cl 178.53(2). For **2**: Co−Si 2.2262(9), Co−P1 2.3684(8), Co−P2 2.3080(9), Co−P3 2.2734(8), Co−Cl 2.3091(8), P1−Co−P2 110.16(3), P1−Co−P3 131.26(3), P2−Co−P3 114.07(3), Si−Co−Cl 174.16(3). For **3**: Ni−Si 2.2134(9), Ni−P1 2.2980(9), Ni−P2 2.2836(9), Ni−P3 2.2840(9), Ni−Cl 2.3143(9), P1−Ni−P2 117.09(3), P1−Ni−P3 118.66(3), P2−Ni−P3 120.27(3), Si−Ni−Cl 178.59(3).

phosphine donors and creates a far more sterically encumbered binding site. To illustrate this point, space-filling models for the hexaisopropyl tris(phosphino)borate and tris(phosphino)silyl iron(II) chloride complexes [PhBP$^{iPr}_3$]-FeCl[20] and [SiP$^{iPr}_3$]FeCl (**6**) are provided in Figure 4. The figure reveals a substantially more protected chloride ligand for the case of **6**.[23] A comparison of the solid-state molecular structures of these complexes reveals slightly shorter Fe−P bonds for complex **6** (Fe−P_{avg} = 2.35 Å) relative to [PhBP$^{iPr}_3$]FeCl (Fe−P_{avg} = 2.43 Å), consistent with the lower spin state of **6** (doublet versus quartet). Thus, it may be possible to ascribe the slightly longer Fe−Cl bond in **6** (2.28 Å versus 2.22 Å for [PhBP$^{iPr}_3$]FeCl) at least in part to the presence of a *trans*-disposed silyl donor. In any case, the steric properties of the tris(phosphino)silyl ligands, combined with the relatively soft nature of the donors, suggest that monovalent, monomeric dinitrogen adducts might be generally accessible.[9b]

Electrochemical Characterization of Divalent Iron and Cobalt Complexes. Comparative cyclic voltammetry data for the divalent iron complexes [SiP$^{iPr}_3$]FeCl (**6**) and [SiP$^{Ph}_3$]FeCl (**8**) are shown in Figure 5 and establish a reversible $Fe^{III/II}$ redox couple for each complex. The oxidation of divalent **6** occurs at $E_{1/2}$ = −670 mV, a 270 mV cathodic shift relative to the phenyl-substituted derivative **8** ($E_{1/2}$ = −400 mV). This difference was anticipated because of the greater electron-releasing character of alkyl versus aryl phosphines, and a similar magnitude shift has been observed for the $Fe^{II/I}$ couple upon substitution of isopropyl for phenyl substituents in tris(phosphino)borate systems.[20]

Complexes **6** and **8** display quite different behavior in their cyclic voltammograms when scanned cathodically under N_2. Whereas phenyl-substituted complex **8** displays a reversible $Fe^{II/I}$ redox couple ($E_{1/2}$ = −2.10 V; Figure 5c), the reduction of complex **6** at E_{max} = −2.55 V is not fully reversible and

Scheme 3

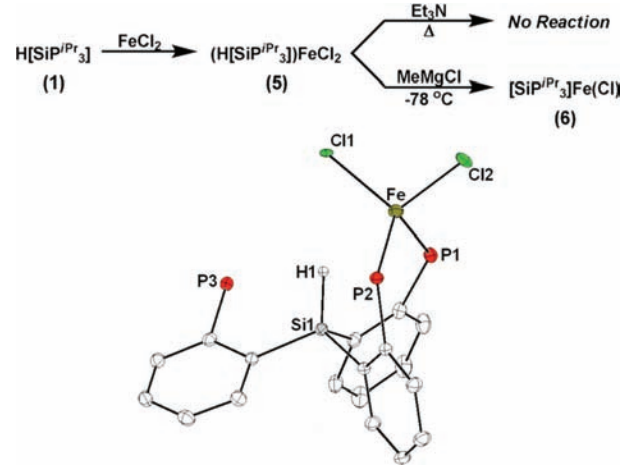

instead appears to generate three distinct products, even at scan rates as fast as 500 mV/s, whose respective oxidations can be seen at −2.40, −2.14, and −1.04 V on the return scan (Figure 5a). To shed light on the identities of these species, complex **6** was subjected to electrochemical interrogation in the absence of N_2 (Figure 5b), and under these conditions both the $Fe^{III/II}$ and $Fe^{II/I}$ couples were found to be reversible and no other species were observed. In light of our previously reported electrochemical results,[9b] we assign the anodic wave observed −2.40 V to the reoxidation of {[SiP$^{iPr}_3$]FeCl}$^-$ and the wave at −1.04 V to the oxidation

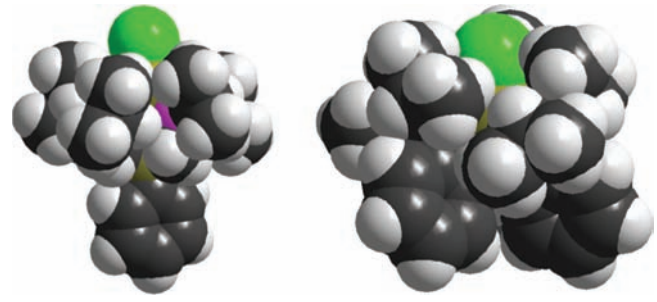

Figure 4. Space-filling models of [PhBP$^{iPr}_3$]FeCl (left) and [SiP$^{iPr}_3$]FeCl (**6**; right); [PhBP$^{iPr}_3$] = [PhB(CH$_2$P^{i}Pr$_2$)$_3$]$^-$.

(22) MacBeth, C. E.; Thomas, J. C.; Betley, T. A.; Peters, J. C. *Inorg. Chem.* **2004**, *43*, 4645.
(23) We have previously provided a similar comparison of the [PhBP$_3$] and [SiP$^{Ph}_3$] ligands (ref 9b).

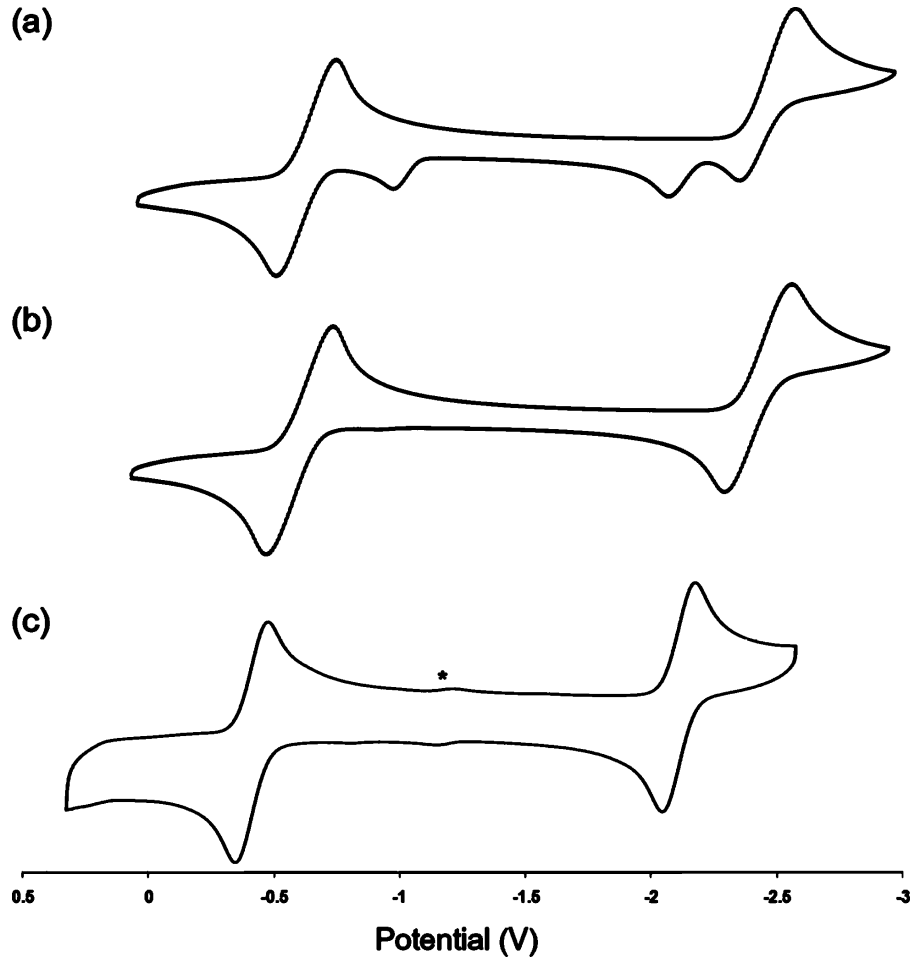

Figure 5. Cyclic voltammograms of (a) [SiP$^{i\mathrm{Pr}}_3$]FeCl (**6**) under N_2, (b) [SiP$^{i\mathrm{Pr}}_3$]FeCl (**6**) under Ar, and (c) [SiP$^{\mathrm{Ph}}_3$]FeCl (**8**) under N_2 (* denotes a trace impurity in **8**). Scans (a) and (b) were recorded at a scan rate of 500 mV/s, and scan (c) was recorded at 100 mV/s. All data were acquired in THF and potentials are referenced to Fc/Fc^+.

of monovalent [SiP$^{i\mathrm{Pr}}_3$]Fe(N_2) (**10**) to its cation, {[SiP$^{i\mathrm{Pr}}_3$]-Fe(N_2)}$^+$. These results also indicate that the species which is oxidized at −2.14 V is generated only in the presence of N_2. Thus, since the position of the anodic wave is consistent with a solvento [SiP$^{i\mathrm{Pr}}_3$]Fe(THF) or a chloride-dissociated "[SiP$^{i\mathrm{Pr}}_3$]Fe" complex,[24] the fact that the species is only observed under N_2 may indicate that chloride loss from {[SiP$^{i\mathrm{Pr}}_3$]FeCl}$^-$ occurs by an associative, N_2-assisted mechanism. Since this hypothesis would invoke an unstable 19-electron intermediate complex, further studies will be required to definitively assign this species.

Figure 6 shows related voltammetry data for the [SiP$^{\mathrm{R}}_3$]CoCl derivatives (R = ^{i}Pr (**2**) or Ph (**9**)), where **9** can be prepared in a fashion analogous to **2**. As with the iron systems, both complexes exhibit reversible $Co^{III/II}$ redox couples with the half-wave potential for **2** ($E_{1/2}$ = −710 mV) being about 260 mV negative of that for **9** ($E_{1/2}$ = −450 mV). Additionally, while **9** exhibits a quasi-reversible $Co^{II/I}$ event, the electrochemical reduction of **2** is completely irreversible. Both are connected with reoxidation events slightly negative of the III/II couple, consistent with the generation of a new Co(I) species by halide expulsion. By analogy with **6**, we assign the new waves to [SiP$^{\mathrm{R}}_3$]Co(N_2) complexes in each case. This assignment is supported by the observation that, as with complex **6** (vide supra), electrochemical reduction of **9** in the absence of N_2 is fully reversible, and the oxidation wave ascribed to the [SiP$^{\mathrm{Ph}}_3$]-Co(N_2) species is no longer present. Interestingly, neither **2** nor **9** displays electrochemical evidence for the generation of an alternative species such as that observed for the [SiP$^{i\mathrm{Pr}}_3$]Fe system.

As with all of the iron and cobalt complexes described, cyclic voltammetry of [SiP$^{i\mathrm{Pr}}_3$]NiCl (**3**) revealed a reversible $Ni^{III/II}$ redox couple ($E_{1/2}$ = −245 mV), indicating that chemical oxidation of this complex should be relatively facile. However, as expected for an 18-electron complex, **3** was not well-behaved upon electrochemical reduction.

Chemical Reduction to Generate Monovalent [SiP$^{i\mathrm{Pr}}_3$]-M(N_2) (M = Fe, Co, Ir). At the outset of our work, it was not clear whether a strongly *trans*-influencing silyl ligand would support a coordinated dinitrogen ligand in a position *trans* to the silyl linkage. Indeed, there have been few examples of M−N_2 complexes that also feature a supporting silyl ligand.[25] None of these contains an N_2 ligand and silyl donor in a *trans* orientation.

(24) A similarly dramatic shift in redox potential upon binding of N_2 at an available Mo(III) coordination site has been described by Peters et al. Peters, J. C.; Cherry, J. P. F.; Thomas, J. C.; Baraldo, L.; Mindiola, D. J.; Davis, W. M.; Cummins, C. C. *J. Am. Chem. Soc.* **1999**, *121*, 10053.

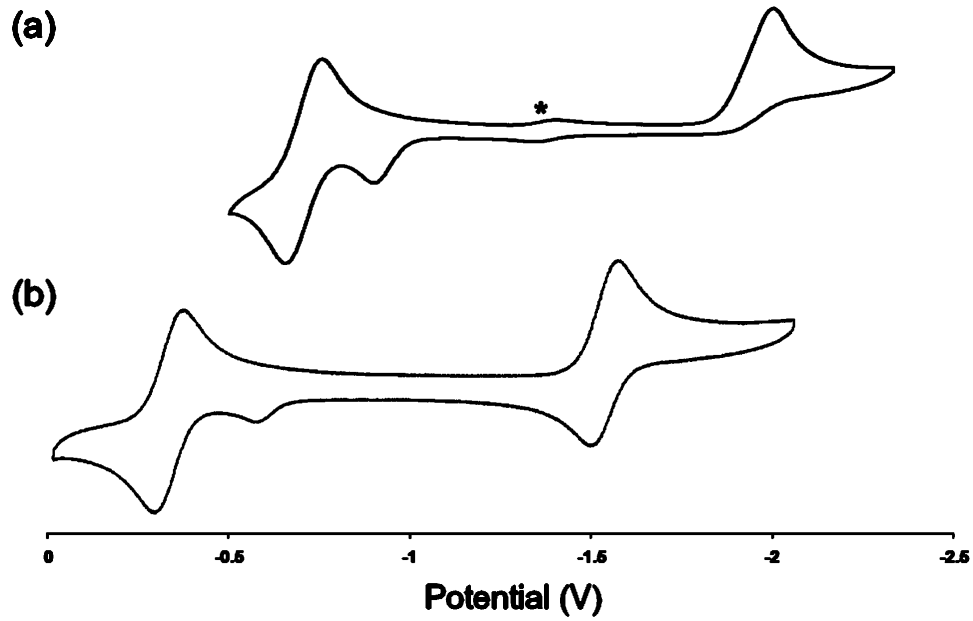

Figure 6. Cyclic voltammograms of (a) [SiP$^{i\text{Pr}}_3$]CoCl (**2**) and (b) [SiP$^{\text{Ph}}_3$]CoCl (**9**) recorded at a scan rate of 100 mV/s (* denotes a trace impurity in **2**). Both scans were recorded in THF under an N_2 atmosphere. Potentials are referenced to Fc/Fc$^+$.

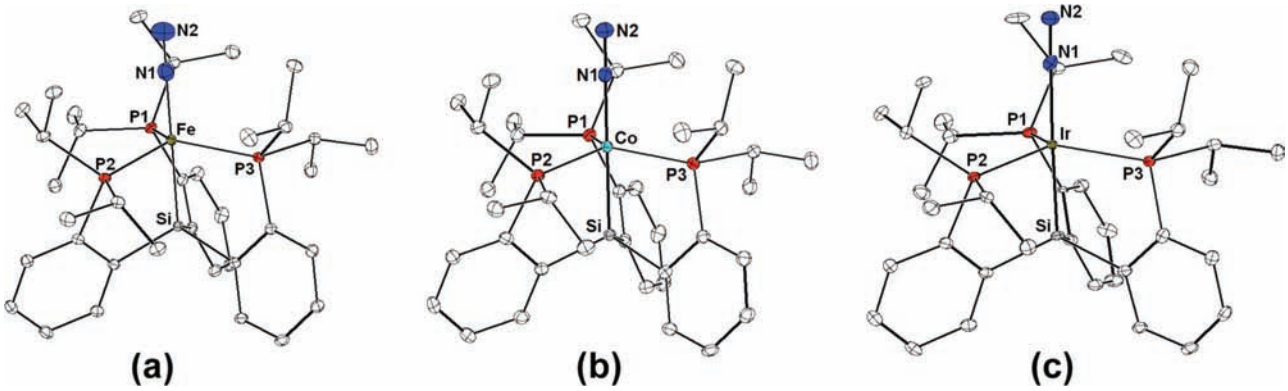

Figure 7. Displacement ellipsoid (35%) representations of (a) [SiP$^{i\text{Pr}}_3$]Fe(N_2) (**10**),[26] (b) [SiP$^{i\text{Pr}}_3$]Co(N_2) (**12**), and (c) [SiP$^{i\text{Pr}}_3$]Ir(N_2) (**14**). Hydrogen atoms and solvent molecules have been omitted for clarity. Selected bond distances (Å) and angles (deg), for **10**: Fe−Si 2.2918(6), Fe−P1 2.3174(5), Fe−P2 2.2954(5), Fe−P3 2.3078(5), Fe−N1 1.817(4), N1−N2 1.065(5), P1−Fe−P2 115.14(1), P1−Fe−P3 119.18(2), P2−Fe−P3 117.82(2), Si−Fe−N1 178.83(6). For **12**: Co−Si 2.2327(6), Co−P1 2.2376(6), Co−P2 2.2277(6), Co−P3 2.2342(6), Co−N1 1.813(2), N1−N2 1.123(3), P1−Co−P2 117.48(2), P1−Co−P3 118.01(2), P2−Co−P3 119.51(2), Si−Co−N1 179.13(6). For **14**: Ir−Si 2.304(2), Ir−P1 2.336(2), Ir−P2 2.328(2), Ir−P3 2.315(2), Ir−N1 2.033(4), N1−N2 1.094(4), P1−Ir−P2 116.00(4), P1−Ir−P3 121.61(6), P2−Ir−P3 117.31(5), Si−Ir−N1 177.05(9).

Exposure of [SiP$^{i\text{Pr}}_3$]FeCl (**6**) to an equivalent of sodium naphthalide results in an immediate darkening of the bright orange solution and the appearance of a prominent infrared stretch (υ_{NN} = 2008 cm^{-1}) consistent with a terminal dinitrogen ligand. NMR and XRD analyses reveal the desired S = 1/2 terminal N_2 complex, [SiP$^{i\text{Pr}}_3$]Fe(N_2) (**10**) (Figure 7).[26] The hexaphenyl complex **8** can be reduced in the same fashion, though the reaction is effected by a weaker reductant (Na/Hg amalgam), consistent with the cyclic voltammetry data. The resulting N_2 complex, [SiP$^{\text{Ph}}_3$]Fe(N_2) (**11**), reveals an intense infrared stretch at higher energy (υ_{NN} = 2041 cm^{-1}), indicating that the N_2 ligand is coordinated to a substantially less electron-rich metal center in this complex. Complexes **10** and **11** are the first examples of d^7 iron complexes containing terminally bonded dinitrogen ligands. The synthesis and structure of **11** was recently communicated.[9b]

The cobalt complexes [SiP$^{i\text{Pr}}_3$]CoCl (**2**) and [SiP$^{\text{Ph}}_3$]CoCl (**9**) are reduced by Na/Hg amalgam in a similar fashion to afford the diamagnetic d^8 dinitrogen complexes [SiP$^{i\text{Pr}}_3$]-Co(N_2) (**12**) and [SiP$^{\text{Ph}}_3$]Co(N_2) (**13**). Again, the N_2 stretching frequencies provide a quantitative measure of the relative electron-releasing properties of each ligand, as a 32 cm^{-1} difference is observed between **12** (υ_{NN} = 2063 cm^{-1}) and **13** (υ_{NN} = 2095 cm^{-1}).

Since divalent iridium halide complexes of [SiP$^{i\text{Pr}}_3$] were not readily available, a somewhat different synthetic strategy was required to access the Ir$^{\text{I}}$−N_2 complex. In a reaction reminiscent of that utilized by Stobart and co-workers to

(25) (a) Dioumaev, V. K.; Plossl, K.; Carroll, P. J.; Berry, D. H. *J. Am. Chem. Soc.* **1999**, *121*, 8391. (b) Yoo, H.; Carroll, P. J.; Berry, D. H. *J. Am. Chem. Soc.* **2006**, *128*, 6038. (c) Trovitch, R. J.; Lobkovsky, E.; Chirik, P. J. *Inorg. Chem.* **2006**, *45*, 7252. (d) Gusev, D. G.; Fontaine, F. G.; Lough, A. J.; Zargarian, D. *Angew. Chem., Int. Ed.* **2003**, *42*, 216.

(26) Compound **10** co-crystallized with a small amount of [SiP$^{i\text{Pr}}_3$]FeCl (**6**) (refined to 4% occupancy). In Figure 8, the chloride ligand (which was refined isotropically because of low occupancy) has been omitted.

Scheme 4

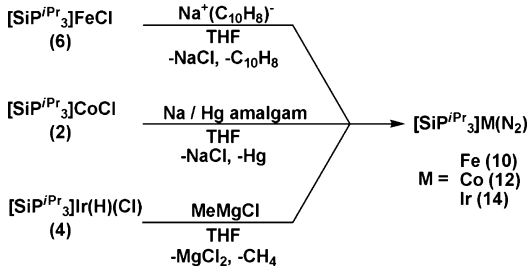

prepare the tris(phosphinoalkyl)silyl rhodium monocarbonyl $((Ph_2PCH_2CH_2)_3Si)Rh(CO)$,[11] [SiP$^{iPr}_3$]Ir(H)(Cl) (**4**) was found to react with 1 equiv of methyl Grignard under a dinitrogen atmosphere to afford the diamagnetic N_2 adduct [SiP$^{iPr}_3$]-Ir(N_2) (**14**) (Scheme 4). The presence of **14** was indicated by a single resonance in the ^{31}P NMR spectrum (δ 38.7 ppm) and an intense N_2 infrared stretch (υ_{NN} = 2122 cm^{-1}). Its identity was confirmed by XRD analysis, revealing a structurally unusual example of a trigonal bipyramidal dinitrogen adduct of iridium(I) (Figure 7).[27]

Table 1 summarizes some pertinent parameters for the N_2 adducts **10**−**14** reported here and related literature compounds.

Having prepared the desired dinitrogen complexes of iron, cobalt, and iridium, we briefly canvassed the lability of the N_2 unit. Early evidence that the *trans* silyl donor would serve to labilize the bound dinitrogen ligand came from the results of combustion analysis data, which consistently indicated lower levels of nitrogen than expected for the empirical formulas of **10**−**14** (between 25% and 50% of the values predicted for the monomeric N_2 complexes). This lability is particularly evident for [SiP$^{iPr}_3$]Ir(N_2) (**14**), where N_2 loss is quickly apparent upon application of vacuum by a color change of the solution from light yellow to dark green. This change in color is reversed upon reintroduction of nitrogen, both in solution and in the solid state. While it is possible that application of vacuum results in the formation of the μ-N_2 dimer species {[SiP$^{iPr}_3$]Ir}$_2$(μ-N_2), similar to complexes known for rhodium and iridium pincer systems,[28] the sterically crowded environment of the binding site in the resulting species would likely prevent dimerization. Instead we suspect that the favored species is a four-coordinate, trigonal pyramidal iridium(I) complex. No direct characterization data is yet in hand, however.

Displacement of the N_2 ligand by CO addition was examined for the case of [SiP$^{iPr}_3$]Co(N_2) (**12**). Thus, exposure of **12** to an atmosphere of carbon monoxide resulted in the rapid and quantitative consumption of the N_2 complex with the appearance of a single new species, [SiP$^{iPr}_3$]Co(CO) (**15**), characterized by ^{31}P NMR (δ 78.2 ppm), IR spectroscopy (υ_{CO} = 1896 cm^{-1}), and XRD analysis (Figure 8). Additionally, oxidation of **12** with silver triflate (either 1 or 2 equiv) effected N_2 loss as evident by infrared spectroscopy and the concomitant formation of either the Co(II) or Co(III) triflato complexes. The cobalt(III) complex {[SiP$^{iPr}_3$]Co(OTf)}{OTf} (**16**) was thoroughly characterized, and XRD analysis (Figure 8) revealed a trigonal bipyramidal complex with one coordinated (κ^1) and one uncoordinated triflate anion. The reluctance of the second triflate ligand to bind, which would afford an octahedral, 18-electron complex, can likely be ascribed to the steric bulk enshrouding the cobalt ion. The utility of this complex as a Co(III) synthon is currently under exploration.

Related chemistry is also prevalent for the iron system. For instance, we have communicated that [SiP$^{Ph}_3$]Fe(N_2) reacts with CO rapidly to afford the terminal carbonyl [SiP$^{Ph}_3$]Fe(CO) (υ_{CO} = 1881 cm^{-1}).[9b] [SiP$^{Ph}_3$]Fe(N_2) can also be oxidized by AgOTf to provide the divalent, structurally characterized triflato species [SiP$^{Ph}_3$]Fe(OTf) (**17**) with release of N_2 (Figure 8).

III. Conclusions

We have described synthetic methods and characterization data for a family of complexes supported by tetradentate tris(phosphino)silyl ligands. In particular, we have introduced the newly prepared hexaisopropyl [SiP$^{iPr}_3$] ligand and characterized several coordination complexes derived from this scaffold. The collective spectroscopic and electrochemical data available indicate that, as expected, [SiP$^{iPr}_3$] is considerably more electron-rich than the related hexaphenyl [SiP$^{Ph}_3$] derivative, whose synthesis was recently communicated.[9b] Importantly, complementary strategies for the installation of the M−Si linkage on later transition metals have been developed, and these strategies provide access to [SiP$^{R}_3$] complexes of iron, cobalt, nickel, and iridium. Reduction of the di- and trivalent [SiP$^{R}_3$]M halide complexes also provides access to unusual trigonal bipyramidal dinitrogen adducts of monovalent iron, cobalt, and iridium, and in all three cases the N_2 ligand appears to be labilized by a strongly *trans*-influencing silyl donor. The propensity of the [SiP$^{R}_3$] ligand to give rise to a single and labile reaction site is one we hope to exploit in the context of future reactivity studies. Specifically, it will be of interest to examine group transfer reactions to both the mid- and low-valent synthons described.

Experimental Section

All manipulations were carried out using standard Schlenk or glovebox techniques under a dinitrogen atmostphere. Unless otherwise noted, solvents were deoxygenated and dried by thorough sparging with N_2 gas followed by passage through an activated alumina column. Non-halogenated solvents were typically tested

(27) Collman, J. P.; Kubota, M.; Vastine, F. D.; Sun, J. Y.; Kang, J. W. *J. Am. Chem. Soc.* **1968**, *90*, 5430.
(28) (a) Cohen, R.; Rybtchinski, B.; Gandelman, M.; Rozenberg, H.; Martin, J. M. L.; Milstein, D. *J. Am. Chem. Soc.* **2003**, *125*, 6532. (b) van der Boom, M. E.; Liou, S. Y.; Ben-David, Y.; Shimon, L. J. W.; Milstein, D. *J. Am. Chem. Soc.* **1998**, *120*, 6531. (c) Ghosh, R.; Kanzelberger, M.; Emge, T. J.; Hall, G. S.; Goldman, A. S. *Organometallics* **2006**, *25*, 5668.
(29) (a) Evans, D. F. *J. Chem. Soc.* **1959**, 2003. (b) Sur, S. K. *J. Magn. Reson.* **1989**, *82*, 169.
(30) George, T. A.; Rose, D. J.; Chang, Y. D.; Chen, Q.; Zubieta, J. *Inorg. Chem.* **1995**, *34*, 1295.
(31) Bianchini, C.; Mealli, C.; Meli, A.; Peruzzini, M.; Zanobini, F. *J. Am. Chem. Soc.* **1988**, *110*, 8725.
(32) Lee, D. W.; Kaska, W. C.; Jensen, C. M. *Organometallics* **1998**, *17*, 1.
(33) Gutierrez-Puebla, E.; Monge, A.; Nicasio, M. C.; Perez, P. J.; Poveda, M. L.; Carmona, E. *Chem.—Eur. J.* **1998**, *4*, 2225.

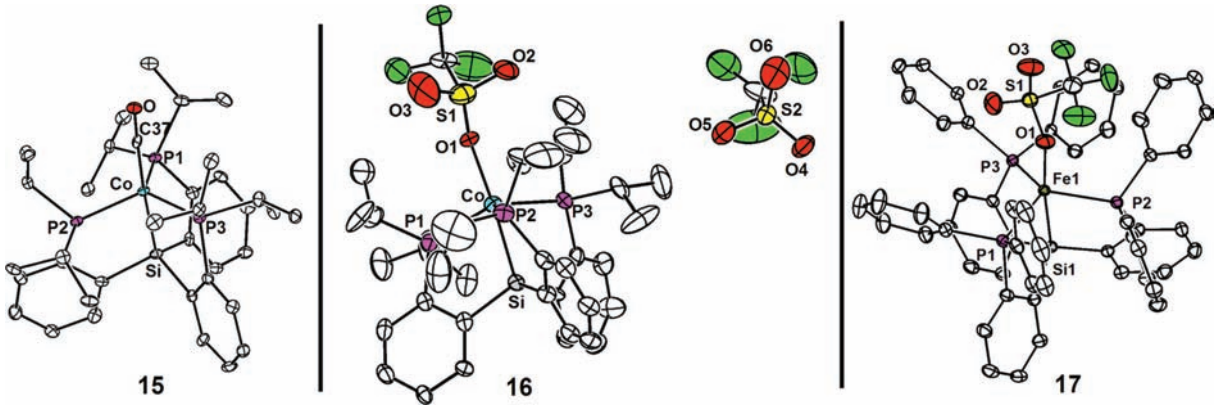

Figure 8. Displacement ellipsoid (35%) representations of [SiP$^{iPr}_3$]Co(CO) (**15**), {[SiP$^{iPr}_3$]Co(OTf)}{OTf} (**16**), and [SiP$^{Ph}_3$]Fe(OTf) (**17**). All hydrogen atoms and co-solvent molecules omitted for clarity. See combined cif file (Supporting Information) for details.

Table 1. Representative Dinitrogen Stretching Frequencies for Complexes of Fe, Co, and Ir

entry	complex	υ_{NN} (cm^{-1})	reference
1	[SiP$^{Ph}_3$]Fe(N$_2$) (**11**)	2041	this work
2	[SiP$^{iPr}_3$]Fe(N$_2$) (**10**)	2008	this work
3	[SiP$^{Ph}_3$]Co(N$_2$) (**13**)	2095	this work
4	[SiP$^{iPr}_3$]Co(N$_2$) (**12**)	2063	this work
5	[SiP$^{iPr}_3$]Ir(N$_2$) (**14**)	2122	this work
6	[NP$^{Ph}_3$]Fe(N$_2$)	1967	30
7	{[NP$^{Ph}_3$]Fe(H)(N$_2$)}$^+$	2090	28
8	{[NP$^{iPr}_3$]Fe(H)(N$_2$)}$^+$	2090	7
9	{[PP$_3$]Co(N$_2$)}$^+$	2128	31
10	IrCl(N$_2$)(C$_8$H$_{12}$O$_4$)(PPh$_3$)$_2$	2190	27
11	[PCP]Ir(N$_2$)	2078	32
12	[Tp*]Ir(Ph)$_2$(N$_2$)	2190	33

[a] [NP$^R_3$] = N(CH$_2$CH$_2$PR$_2$)$_3$. [b] [PP$_3$] = P(CH$_2$CH$_2$PPh$_2$)$_3$. [c] [PCP] = C$_6$H$_3$-2,6-(CH$_2$P^{t}Bu$_2$)$_2$. [d] [Tp*] = tris(3,5-dimethylpyrazol)yl borate.

with a standard purple solution of sodium benzophenone ketyl in tetrahydrofuran to confirm effective oxygen and moisture removal. (2-bromophenyl)diisopropylphosphine[12] and (2-bromophenyl)diphenylphosphine[9a] were prepared according to literature procedures. All other reagents were purchased from commercial vendors and used without further purification unless otherwise noted. Deuterated solvents were purchased from Cambridge Isotopes Laboratories, Inc. and were degassed and stored over activated 3 Å molecular sieves prior to use.

Physical Methods. Elemental analyses were performed by Desert Analytics, Tucson, AZ. A Varian Mercury-300 spectrometer was used to record ^{1}H, ^{31}P{^{1}H}, and ^{13}C{^{1}H} spectra at room temperature unless otherwise noted. ^{1}H and ^{13}C{^{1}H} chemical shifts were referenced to residual solvent. ^{31}P{^{1}H} NMR are reported relative to an external standard of 85% H_3PO_4 (0 ppm). Abbreviations for reported signal multiplicities are as follows: s, singlet; d, doublet; t, triplet; q, quartet; m, multiplet; br, broad. IR spectra were recorded on a Bio-Rad Excalibur FTS 3000 spectrometer controlled by Win-IR Pro software using a KBr solution cell. Solution magnetic moments were measured at 298 K following the Evans method.[29] UV−vis measurements were recorded on a Varian Cary 50 Bio Spectrophotometer controlled by Cary WinUV Software. All measurements were recorded using a quartz cell fitted with a Teflon cap. XRD studies were carried out in the Beckman Institute Crystallographic Facility on a Bruker Smart 1000 CCD diffractometer. Electrochemical analysis was performed on a CHI 600B Potentiostat/Galvanostat using a glassy carbon working electrode, a platinum wire auxiliary electrode, and an Ag/AgNO$_3$ non-aqueous reference electrode filled with THF and Bu_4NPF_6.

X-ray Crystallography Procedures. X-ray quality crystals were grown as indicated in the experimental procedures for each complex. The crystals were mounted on a glass fiber with Paratone N oil. Structures were determined using direct methods with standard Fourier techniques using the Bruker AXS software package. In some cases, Patterson maps were used in place of the direct methods procedure. Table 2 contains the XRD experimental details and CIF files are provided in the Supporting Information.

Tris(o-(diisopropylphosphino)phenyl)silane (H[SiP$^{iPr}_3$], 1). (2-Bromophenyl)diisopropylphosphine (4.1429 g, 15.164 mmol) was dissolved in 100 mL of diethyl ether and chilled to −78 °C, and *n*-butyllithium (1.60 M in hexanes, 9.50 mL, 15.2 mmol) was added dropwise, causing a darkening of the mixture and gradual precipitation of solids. After 15 min, the slurry was brought to room temperature and stirred for 2 h, after which volatiles were removed in vacuo to yield a pale red powder. The powder was redissolved in toluene (80 mL), chilled to −35 °C, and trichlorosilane (511 μL, 5.06 mmol) was added in one portion, resulting in the immediate precipitation of white solids and lightening of the solution. The mixture was stirred at room temperature for 30 min, then at 90 °C for 15 h, and filtered through Celite to give a clear, light orange solution. Solvents were removed in vacuo to give an orange oil, and the addition of petroleum ether (20 mL) caused the precipitation of white solids. These were isolated on a frit and washed with petroleum ether (2 × 5 mL) to yield **1** as a white powder. Subsequent crops could be isolated by crystallization from concentrated petroleum ether solutions at −35 °C (0.5439 g, 18%). ^{1}H NMR (C$_6$D$_6$): δ 7.46−7.34 (m, 3H, Ar−*H*). 7.30−7.20 (m, 3H, Ar−*H*), 7.20−7.10 (td, *J* = 1.2 and 7.2 Hz, 3H, Ar−*H*), 7.02−6.92 (tt, *J* = 1.5 and 7.5 Hz, 3H, Ar−*H*), 2.05−1.85 (doublet of septets, $^2J_{HP}$ = 6.9 Hz, $^3J_{HH}$ = 3.0 Hz, 6H, −C*H*(CH$_3$)$_2$), 1.20−1.02 (m, 18H, −CH(C*H*$_3$)$_2$), 1.00−0.88 (m, 18H, −CH(C*H*$_3$)$_2$). ^{31}P NMR (C$_6$D$_6$): δ 1.7 (s). IR (THF, KBr, cm^{-1}) υ(Si−H): 2218. Anal. Calcd for C$_{36}$H$_{55}$P$_3$Si: C, 71.02; H, 9.11. Found: C, 71.09; H, 9.38.

[SiP$^{iPr}_3$]CoCl (2). H[SiP$^{iPr}_3$] (102.6 mg, 0.1685 mmol) and triethylamine (100 μL, 1.35 mmol) were dissolved in THF (5 mL) and added by pipet to a stirring solution of cobaltous chloride (21.9 mg, 0.169 mmol) in THF (10 mL), causing an immediate color change from light blue to dark green. Over a period of 30 min, the solution gradually adopted a maroon hue and was allowed to stir 12 h. Volatiles were removed in vacuo, and the residues extracted into diethyl ether (15 mL), filtered, and dried to an analytically pure red powder (95.2 mg, 80%). Crystals suitable for XRD were grown by slow evaporation of benzene from a concentrated solution. ^{1}H NMR (C$_6$D$_6$): δ 8.7, 8.0, 7.8, 7.4, 7.3, 6.7, 2.8, 2.6, 2.3, 1.6,

Table 2. XRD Experimental Details for **1**, **2**, **3**, **4**, **5**, **6**, **10**, **12**, **14**, **15**, and **16**

	1	**2**	**3**	**4**	**5**	**6**	**10**	**12**	**14**	**15**	**16**	**17**
chemical formula	$C_{36}H_{55}P_3Si$	$C_{36}H_{54}ClCoP_3Si$	$C_{42}H_{60}ClNiP_3Si$	$C_{36}H_{55}ClIrP_3Si\cdot C_6H_6$	$C_{36}H_{55}Cl_2FeP_3Si$	$C_{36}H_{54}ClFeP_3Si\cdot C_6H_6$	$0.96\ C_{36}H_{54}FeN_2P_3Si\cdot 0.04\ C_{36}H_{54}ClFeP_3Si\cdot C_6H_6$	$C_{36}H_{54}CoN_2P_3Si\cdot C_6H_6$	$C_{36}H_{54}IrN_2P_3Si$	$C_{37}H_{54}CoOP_3Si$	$C_{38}H_{54}CoF_6O_4P_3S_2Si$	$C_{59}H_{58}FeF_3O_3P_3SSi$
formula weight	608.80	702.17	780.06	914.56	735.55	777.20	769.77	694.74	828.01	694.73	964.86	1088.91
T (°C)	−173	−173	−173	−173	−173	−173	−173	−173	−173	−173	−173	−173
λ (Å)	0.71073	0.71073	0.71073	0.71073	0.71073	0.71073	0.71073	0.71073	0.71073	0.71073	0.71073	0.71073
a (Å)	11.3718(3)	16.149(5)	12.916(4)	19.5771(15)	13.0548(19)	12.913(4)	12.759(2)	12.6932(9)	15.98(2)	16.13(2)	10.8159(10)	22.7568(7)
b (Å)	11.5291(4)	17.085(4)	15.540(3)	11.0445(9)	13.718(3)	15.513(4)	15.4865(19)	15.4021(11)	17.151(12)	17.050(14)	14.3316(13)	16.8912(5)
c (Å)	c = 16.4561(5)	25.497(6)	20.130(5)	18.5937(14)	22.356(6)	20.296(8)	20.561(4)	20.6008(15)	25.95(2)	25.54(2)	28.152(3)	26.7730(8)
α (deg)	96.135(2)	90	90	90	90	90	90	90	90	90	90	90
β (deg)	105.964(2)	90	92.32(3)	90	104.102(11)	92.33(3)	92.006(16)	91.9160(10)	90	90	90	90
γ (deg)	116.084(2)	90	90	90	90	90	90	90	90	90	90	90
V (Å^3)	1797.0(1)	7035(3)	4037(2)	4020.3(5)	3883.0(13)	4062(2)	4060.1(11)	4025.2(5)	7115(12)	7023(13)	4363.9(7)	10291.3(5)
space group	$P\bar{1}$	*Pbca*	*P*2(1)/*c*	*Pna*2(1)	*P*2(1)/*n*	*P*2(1)/*c*	*P*2(1)/*c*	*P*2(1)/*c*	*Pbca*	*Pbca*	*P*2(1)2(1)2(1)	*Pbca*
Z	2	8	4	4	4	4	4	4	8	8	4	8
D_{calcd} (g/cm^3)	1.125	1.326	1.283	1.511	1.258	1.271	1.259	1.275	1.546	1.314	1.469	1.406
R1, wR2[a] ($I > 2\sigma(I)$)	0.0722, 0.1839	0.0546, 0.0877	0.0509, 0.0820	0.0385, 0.0758	0.0688, 0.2052	0.0510, 0.0872	0.0521, 0.1287	0.0475, 0.1050	0.0496, 0.0767	0.0707, 0.1150	0.0783, 0.1895	0.0598, 0.1229

[a] $R1 = \sum||F_o| - |F_c||/\sum|F_o|$, $wR2 = \{\sum[w(F_o^2 - F_c^2)^2]/\sum w(F_o^2)^2\}^{1/2}$.

1.4, 1.2, 1.0, 0.6. UV−vis (THF) λ_{max}, nm (ε, M^{-1} cm^{-1}): 508 (1100), 420 (1700). μ_{eff} (C_6D_6): 1.8 μ_B. Anal. Calcd for $C_{36}H_{54}ClCoP_3Si$: C, 61.58; H, 7.75. Found: C, 61.29; H, 7.61.

[SiP$^{i\mathrm{Pr}}_3$]NiCl (3). To a stirring slurry of nickel(II) chloride in THF (5 mL) was added a solution of H[SiP$^{i\mathrm{Pr}}_3$] (34.5 mg, 0.0567 mmol) in THF (3 mL). Triethylamine (ca. 200 μL) was added and the solution was heated at reflux for 12 h with stirring, causing a color change to bright red. Volatiles were removed *in vacuo* and the residues extracted into benzene (5 mL), filtered through Celite and lyophilized to yield **3** as a pale red powder (38.0 mg, 96%). Crystals suitable for XRD were grown by slow evaporation of benzene from a concentrated solution. ^{1}H NMR (C_6D_6): δ 7.78−7.70 (m, 3H, Ar−*H*), 7.30−7.24 (m, 6H, Ar−*H*), 7.15−7.00 (m, 3H, Ar−*H*), 2.70−2.55 (m, 6H, −C*H*(CH$_3$)$_2$), 1.35−1.20 (m, 18H, −CH(C*H*$_3$)$_2$), 1.00−0.80 (m, 18H, −CH(C*H*$_3$)$_2$). ^{31}P NMR (C_6D_6): δ 35.6 (s). UV−vis (THF) λ_{max}, nm (ε, M^{-1} cm^{-1}): 482 (1500), 349 (2000). Anal. Calcd for $C_{36}H_{54}ClNiP_3Si$: C, 61.60; H, 7.75. Found: C, 61.55; H, 7.73.

[SiP$^{i\mathrm{Pr}}_3$]Ir(H)(Cl) (4). To a stirring solution of [(cod)IrCl]$_2$ (60.1 mg, 0.0895 mmol) was added a solution of H[SiP$^{i\mathrm{Pr}}_3$] (108.8 mg, 0.1787 mmol) in THF (3 mL), causing an immediate color change from orange to yellow. After 12 h, volatiles were removed in vacuo, and the residues dissolved in benzene (10 mL), filtered through Celite, and lyophilized to yield **4** as a pale yellow powder (142.4 mg, 95%). Analytically pure sample was obtained as colorless crystals by vapor diffusion of petroleum ether into a concentrated benzene solution, and analysis is reported for **4**·(C_6H_6). ^{1}H NMR (C_6D_6): δ 8.10 (d, J = 7.2 Hz, 2H, Ar−*H*), 7.92 (d, J = 6.9 Hz, 1H, Ar−*H*), 7.38−7.28 (m, 2H, Ar−*H*), 7.26−7.20 (m, 1H, Ar−*H*), 7.14−6.94 (m, 6H, Ar−*H*), 3.00−2.85 (m, 2H, −C*H*(CH$_3$)$_2$), 2.80−2.65 (m, 2H, −C*H*(CH$_3$)$_2$), 2.55−2.40 (m, 2H, −C*H*(CH$_3$)$_2$), 1.90−1.75 (m, 6H, −CH(C*H*$_3$)$_2$), 1.45−1.25 (m, 12H, −CH(C*H*$_3$)$_2$), 1.05−0.90 (m, 12H, −CH(C*H*$_3$)$_2$), 0.60−0.45 (m, 6H, −CH(C*H*$_3$)$_2$), −10.83 (dt, $^2J_{HP(trans)}$ = 118 Hz, $^2J_{HP(cis)}$ = 24 Hz, 1H, Ir−*H*). ^{31}P NMR (THF): δ 28.9 (br s, 1P, P−Ir−H$_{trans}$), 25.5 (d, $^2J_{HP}$ = 100 Hz, 2P, P−Ir−H$_{cis}$). UV−vis (THF) λ_{max}, nm (ε, M^{-1} cm^{-1}): 495 (18), 428 (48), 367 (120). IR (THF, KBr, cm^{-1}) υ(Ir−H): 2145. Anal. Calcd for $C_{42}H_{61}ClP_3IrSi$: C, 55.15; H, 6.72. Found: C, 55.11; H, 6.66.

[SiP$^{i\mathrm{Pr}}_3$]FeCl (6). To a stirring slurry of ferrous chloride (30.6 mg, 0.241 mmol) in THF (10 mL) was added a solution of H[SiP$^{i\mathrm{Pr}}_3$] (147.2 mg, 0.2418 mmol) in THF (5 mL), causing a color change to yellow as complex **5** was generated (n.b. Crystalline samples of **5** could be isolated at this point by removal of solvent and crystallization from benzene). The resulting solution was chilled to −78 °C, and MeMgCl (3.0 M in THF, 81 μL, 0.24 mmol) was diluted in THF (1 mL) and added dropwise, causing an immediate darkening of the solution. The reaction was stirred at −78 °C for 1 h, then warmed to room temperature and stirred 3 h to give a dark orange solution. The solution was filtered through Celite and concentrated to an orange film in vacuo. The residues were extracted into benzene, filtered, lyophilized, and washed with petroleum ether (3 × 3 mL) to yield **6** as an orange powder (72.5 mg, 43%). Crystals suitable for XRD were obtained by slow evaporation of benzene from a concentrated solution. ^{1}H NMR (C_6D_6): δ 7.3, 5.4, 2.6, −2.7 ppm. UV−vis (THF) λ_{max}, nm (ε, M^{-1} cm^{-1}): 471 (990), 379 (2100). μ_{eff} (C_6D_6): 3.3 μ_B. Anal. Calcd for $C_{36}H_{54}ClFeP_3Si$: C, 61.85; H, 7.79. Found: C, 62.34; H, 7.96.

Tris(o-(diphenylphosphino)phenyl)silane (H[SiP$^{\mathrm{Ph}}_3$], 7). (2-Bromophenyl)diphenylphosphine (10.24 g, 30.0 mmol) was dissolved in diethyl ether (150 mL) and cooled to −78 °C. *n*-Butyllithium (1.60 M in hexanes,18.8 mL, 30.0 mmol) was added slowly,

giving a light orange solution with a tan-colored precipitate. This mixture was allowed to warm gradually to room temperature and then stirred for 1 h, after which the volatiles were removed in vacuo. Toluene (150 mL) was added, and the cloudy orange solution was cooled back to −78 °C. Trichlorosilane (1.01 mL, 10.0 mmol) was added in one portion, and the resulting mixture was warmed to room temperature gradually. After stirring for 30 min, the reaction was heated in a sealed reaction bomb to 110 °C for 15 h. The resulting yellow solution and white precipitate were cooled to room temperature and filtered through Celite, and the filtrate was concentrated to white solids. Petroleum ether (100 mL) was added, and the resulting mixture was stirred vigorously for 20 min, at which point tan solids were collected on a sintered glass frit and washed with additional petroleum ether (2 × 30 mL) to afford **7** as a fine tan powder (6.15 g, 76%). ^{1}H NMR (C_6D_6): δ 7.63 (dm, J = 1.5 and 6.3 Hz, 3H), 7.34 (ddm, J = 1.0, 3.9, and 7.8 Hz, 3H), 7.25−7.20 (m, 12H), 7.05 (td, J = 1.5 and 7.3 Hz, 6H), 7.02−6.95 (m, 19H). ^{13}C NMR (C_6D_6): δ 145.5 (d, J = 11.4 Hz), 144.3 (t, J = 4.0 Hz), 144.0 (t, J = 4.0 Hz), 138.8 (d, J = 14.6 Hz), 138.5 (d, J = 12.8 Hz), 134.7, 134.5 (d, J = 19.2 Hz), 130.4, 128.8, 128.6 (d, J = 17.3 Hz). ^{31}P NMR (C_6D_6): δ −10.4 (s). IR (KBr, cm^{-1}) υ(Si−H): 2170. Anal. Calcd for $C_{54}H_{43}P_3Si$: C, 79.78; H, 5.33. Found: C, 79.39; H, 5.61.

[SiP$^{Ph}_3$]FeCl (8). H[SiP$^{Ph}_3$] (2.19 g, 2.69 mmol) and $FeCl_2$ (0.341 g, 2.69 mmol) were combined in THF (50 mL) and cooled to −78 °C. *n*-Butyllithium (1.60 M in hexanes, 1.68 mL, 2.69 mmol) was added slowly, resulting in an immediate color change to dark red. The mixture was allowed to warm to room temperature, and after stirring for 2 h was concentrated to oily red solids. Benzene (50 mL) was added, and the resulting solution was filtered through Celite and concentrated. Diethyl ether (40 mL) was added, and the mixture was stirred vigorously, yielding an orange precipitate and a red supernatant. The orange solids were collected on a sintered glass frit and washed with additional diethyl ether portions, yielding pure **8** as a light orange powder (1.28 g, 53%). Crystals suitable for XRD were obtained by slow diffusion of petroleum ether vapors into a dichloromethane solution. ^{1}H NMR (C_6D_6): δ 12.32, 7.61, 6.99, 4.67, 3.29, −2.09, −5.03. μ_{eff} (C_6D_6): 2.9 μ_B. UV−vis (toluene) λ_{max}, nm (ε, M^{-1} cm^{-1}): 479 (5700), 426 (4700). Anal. Calcd for $C_{54}H_{42}ClFeP_3Si$: C, 71.81; H, 4.69. Found: C, 71.82; H, 4.41.

[SiP$^{Ph}_3$]CoCl (9). H[SiP$^{Ph}_3$] (0.483 g, 0.595 mmol) and $CoCl_2$ (0.0830 g, 0.639 mmol) were combined in THF (30 mL) with ^{i}Pr$_2$NEt (110 μL, 0.666 mmol). After several minutes, the blue solution adopted a red hue and was stirred for 16 h. Solvent was removed under reduced pressure, and the remaining solid was dissolved in benzene (30 mL). This solution was filtered through a glass microfilter and lyophilized to yield spectroscopically pure **9** as a fluffy red powder (0.4686 g, 87%). Crystals suitable XRD were obtained by vapor diffusion of petroleum ether into a saturated solution of **9** in methylene chloride. ^{1}H NMR (C_6D_6): δ 10.3, 8.1, 7.7, 5.6, 3.0, −1.2. UV−vis (C_6H_6) λ_{max}, nm (ε, M^{-1} cm^{-1}): 402 (5700), 506 (3800).

As we have noted previously,[9b] complexes **10**−**14** proved unstable to extended exposure to vacuum because of the lability of the N_2 ligand. Although the reported complexes were spectroscopically pure, suitable elemental analyses were not obtained.

[SiP$^{iPr}_3$]Fe(N$_2$) (10). A dark green solution of sodium naphthalide was prepared by stirring a colorless solution of naphthalene (8.6 mg, 0.067 mmol) in THF (3 mL) over excess sodium metal (8.0 mg, 0.35 mmol) for 3 h. The resulting naphthalide solution was filtered away from sodium and added dropwise to an orange solution of **6** (46.8 mg, 0.0669 mmol) in THF (5 mL), causing the color of the solution to change to dark orange over a period of several minutes. The reaction was allowed to proceed overnight, filtered, and volatiles removed in vacuo to give an orange-red film. The residues were extracted into benzene (5 mL), filtered, and dried. The residues were triturated with petroleum ether (1 × 5 mL) to give a red powder that was washed with petroleum ether (2 × 3 mL) to yield spectroscopically pure **10** (10.5 mg, 23%). Crystals suitable for XRD were obtained by slow evaporation of benzene from a concentrated solution. ^{1}H NMR (C_6D_6): δ 10, 7.1, 7.0, 3.8, 2.1, 1.1 ppm. μ_{eff} (C_6D_6): 2.2 μ_B. IR (THF, KBr, cm^{-1}) υ(N$_2$): 2008. UV−vis (THF) λ_{max}, nm (ε, M^{-1} cm^{-1}): 468 (1800), 380 (3500).

[SiP$^{Ph}_3$]Fe(N$_2$) (11). Sodium (8.3 mg, 0.36 mmol) and mercury (0.714 g) were combined in THF (1 mL). Solid **8** (0.322 g, 0.357 mmol) was added, and the total volume was brought up to 15 mL. After vigorous stirring for 6 h at room temperature, a brown supernatant was decanted off the Na/Hg amalgam and concentrated in vacuo to brown solids. Benzene (10 mL) was added, and the resulting cloudy solution was filtered through Celite. The resulting red-orange filtrate was lyophilized, providing spectroscopically pure **11** as a fluffy red-orange solid (0.278 g, 87%). Crystals suitable for XRD were obtained by slow diffusion of petroleum ether vapors into a THF solution. ^{1}H NMR (C_6D_6): δ 10.48, 7.98, 7.42, 6.17, 4.46, −1.85 (br), −1.86. μ_{eff} (C_6D_6): 1.8 μ_B. UV−vis (toluene) λ_{max}, nm (ε, M^{-1} cm^{-1}): 347 (9400). IR (KBr, cm^{-1}) υ(N$_2$): 2041.

[SiP$^{iPr}_3$]Co(N$_2$) (12). A red solution of **2** (154.3 mg, 0.2197 mmol) in THF (10 mL) was added onto a 0.27 weight % Na/Hg amalgam (0.0057 g, 0.25 mmol sodium dissolved in 2.0875 g of mercury) with stirring. Over a period of 2 h, the color of the solution changed from red to golden. After 12 h, the solution was filtered to remove insoluble residues and volatiles were removed in vacuo to give a golden film. The residues were extracted into benzene, filtered, and lyophilized to an orange powder, which was subsequently washed with petroleum ether (3 × 10 mL) to yield **12** as a bright orange powder (90.4 mg, 60%). Crystals suitable for XRD were obtained by slow evaporation of benzene from a concentrated solution. ^{1}H NMR (C_6D_6): δ 7.89 (d, J = 6.9 Hz, 3H, Ar−*H*), 7.21−6.95 (m, 9H, Ar−*H*), 2.51 (br, 6H, −C*H*(CH$_3$)$_2$), 1.11 (br, 18H, −CH(C*H*$_3$)$_2$), 0.65 (br, 18H, −CH(C*H*$_3$)$_2$). ^{31}P NMR (C_6D_6): δ 65.7 (s). IR (THF, KBr, cm^{-1}) υ(N$_2$): 2063. UV−vis (THF) λ_{max}, nm (ε, M^{-1} cm^{-1}): 381 (2800).

[SiP$^{Ph}_3$]Co(N$_2$) (13). A red solution of **9** (0.035 g, 0.039 mmol) in THF (10 mL) was added onto a 0.5 weight % Na/Hg amalgam (0.0015 g, 0.066 mmol sodium dissolved in 0.3025 g of mercury) with stirring, causing a gradual color change to brown. After 12 h, the mixture was decanted from the amalgam and filtered through Celite to give an orange solution. Solvent was removed in vacuo, and the residues were extracted into benzene, filtered, and lyophilized to afford **13** as an orange powder (0.014 g, 45%). ^{1}H NMR (C_6D_6): δ 8.1, 7.4, 7.2, 7.0, 6.9, 6.8. ^{31}P NMR (C_6D_6): δ 63.5. UV−vis (C_6H_6) λ_{max}, nm (ε, M^{-1} cm^{-1}): 378 (2000). IR (KBr, cm^{-1}) υ(N$_2$): 2095.

[SiP$^{iPr}_3$]Ir(N$_2$) (14). A colorless solution of **4** (101.2 mg, 0.1210 mmol) in THF (5 mL) was chilled to −78 °C. MeMgCl (3.0 M in THF, 44 μL, 0.132 mmol) was diluted in 1 mL of THF and added dropwise to the stirring solution. The reaction was allowed to proceed at −78 °C for 30 min with no color change, then warmed to room temperature, and stirred for 4 h, causing a change in color to bright yellow. The mixture was concentrated in vacuo to give a green film which was subsequently extracted into benzene/petroleum ether (2:1, 20 mL). The solution was filtered through

Celite and dried to afford **14** as an electric yellow powder (87.5 mg, 87%). ^{1}H NMR (C_6D_6): δ 8.09 (d, J = 6.9 Hz, 3H, Ar−*H*), 7.30−7.20 (m, 3H, Ar−*H*), 7.20−7.10 (m, 3H, Ar−*H*), 7.10−7.00 (m, 3H, Ar−*H*), 2.52 (br, 6H, −C*H*(CH_3)$_2$), 1.06 (br, 18H, −CH(C*H*$_3$)$_2$), 0.69 (br, 18H, −CH(C*H*$_3$)$_2$). ^{31}P NMR (C_6D_6): δ 38.7 (s). IR (THF, KBr, cm^{-1}) υ(N_2): 2122. UV−vis (THF) λ_{max}, nm (ε, M^{-1} cm^{-1}): 310 (7600).

[SiP$^{i\mathrm{Pr}}_3$]Co(CO) (15). In a sealed NMR tube, an orange solution of **12** in THF (1 mL) was frozen, and the headspace evacuated and backfilled with carbon monoxide. Over a period of 12 h, the hue of the solution lightened from orange to yellow. Consumption of **12** and appearance of **15** was confirmed by NMR and IR, and yellow X-ray quality crystals were grown by storing a concentrated solution of **15** in petroleum ether at −35 °C. ^{31}P NMR (THF): δ 78.2 (s). IR (THF, KBr, cm^{-1}) υ(CO): 1896.

[SiP$^{i\mathrm{Pr}}_3$]Co(OTf)$_2$ (16). To a solution of **12** (45.1 mg, 0.0649 mmol) in THF (5 mL) was added a colorless solution of silver triflate (33.4 mg, 0.130 mmol) in THF (5 mL). The color of the mixture immediately changed from orange to green as it became cloudy. After 5 h, the solution was filtered through Celite and concentrated in vacuo to a green film. The product was triturated with petroleum ether (1 × 5 mL) and washed with petroleum ether (3 × 5 mL) and benzene (1 × 5 mL) to give **16** as a fine green powder (81.0 mg, 84%). X-ray quality crystals were grown by vapor diffusion of petroleum ether into a concentrated solution of **16** in THF. ^{1}H NMR (CD_3CN): δ 11.9, 7.8, 7.4, 7.2, 7.0, 3.8, 3.4, 3.0, 2.7, 1.9, 1.2, 0.9, 0.6, −3.5. UV−vis (THF) λ_{max}, nm (ε, M^{-1} cm^{-1}): 810 (220), 611 (330), 517 (390), 373 (2300). μ_{eff} (THF-d_8): 3.3 μ_B. Anal. Calcd for $C_{38}H_{54}CoF_6O_6P_3S_2Si$: C, 47.30; H, 5.64. Found: C, 47.17; H, 5.73.

[SiP$^{\mathrm{Ph}}_3$]Fe(OTf) (17). In separate scintillation vials, [SiP$^{\mathrm{Ph}}_3$]FeN_2 (29.5 mg, 0.0329 mmol) and AgOTf (8.5 mg, 33 mmol) were dissolved in THF (1 mL each) and cooled to −35 °C. The AgOTf solution was then added slowly to the [SiP$^{\mathrm{Ph}}_3$]FeN_2 solution with stirring. After stirring for 5 h at room temperature, volatiles were removed. Et_2O (10 mL) was added, and black solids were filtered away from the resulting suspension to yield an orange filtrate. Volatiles were removed to yield **17** as an orange powder (22.2 mg, 66%). ^{1}H NMR (C_6D_6, δ): 12.4, 5.4, 5.1, −4.3. μ_{eff} (C_6D_6): 3.0 μ_B. UV−vis (toluene, nm(M^{-1}cm^{-1}): 432(1440), 489(1840). IR (KBr, cm^{-1}): 3050, 2958, 1586, 1482, 1435, 1324, 1232 (OTf), 1210 (OTf), 1179 (OTf), 1108, 1027. Anal. Calcd for $C_{55}H_{42}F_3FeO_3P_3SSi$: C, 64.97; H, 4.16. Found:.C 64.08; H, 3.76.

Acknowledgment. We acknowledge the NIH (GM-070757), the Moore Foundation (fellowship to M.T.W.), and the National Science Foundation (fellowship to N.P.M.). Larry Henling provided crystallographic assistance.

Supporting Information Available: CIF files for complexes **1**−**6**, **10**, **12**, **14**, **15**, **16**, and **17**. This material is available free of charge via the Internet at http://pubs.acs.org.

IC801855Y